

The electron-phonon coupling constant, the Fermi temperature and unconventional superconductivity in the carbonaceous sulfur hydride 190 K superconductor

E. F. Talantsev^{1,2}

¹M.N. Miheev Institute of Metal Physics, Ural Branch, Russian Academy of Sciences,
18, S. Kovalevskoy St., Ekaterinburg, 620108, Russia

²NANOTECH Centre, Ural Federal University, 19 Mira St., Ekaterinburg, 620002,
Russia

E-mail: evgeny.talantsev@imp.uran.ru

Abstract

Recently, Snider *et al* (2020 *Nature* **586** 373) reported on the observation of superconductivity in highly-compressed carbonaceous sulfur hydride, $H_x(S,C)_y$. The highest critical temperature in $H_x(S,C)_y$ by 5 K exceeds previous record of $T_c = 280$ K reported by Somayazulu *et al* (2019 *Phys. Rev. Lett.* **122** 027001) for highly-compressed LaH_{10} . In this paper we analyse experimental temperature dependent magnetoresistance data, $R(T,B)$, reported by Snider *et al*. The analysis shows that $H_x(S,C)_y$ compound exhibited $T_c = 190$ K ($P = 210$ GPa) has the electron-phonon coupling constant $\lambda_{e-ph} = 2.0$ and the ratio of critical temperature, T_c , to the Fermi temperature, T_F , in the range of $0.011 \leq T_c/T_F \leq 0.018$. These deduced values are very close to ones reported for H_3S at $P = 155-165$ GPa (Drozdov *et al* 2015 *Nature* **525** 73). This means that in all considered scenarios the carbonaceous sulfur hydride 190 K superconductor falls into unconventional superconductors band in the Uemura plot, where all other highly-compressed super-hydride/deuterides are located. It should be noted that that our analysis shows that all raw $R(T,B)$ datasets for $H_x(S,C)_y$ samples for which Snider *et al* (2020 *Nature* **586** 373) reported $T_c > 200$ K cannot be characterised as reliable data sources. Thus, independent experimental confirmation/disprove high- T_c values in the carbonaceous sulfur hydride is required.

I. Introduction

In 2015 Drozdov *et al* [1] discovered the first near-room-temperature (NRT) superconductor highly-compressed sulphur hydride, H_3S . To date, NRT superconductivity has been observed in four super-hydrides/deuterides systems subjected to high pressure: Th-H [2], S-(H,D) [1,3-5], Y-H [6,7], La-(H,D) [8-10].

Recently, Snider *et al* [11] reported on the observation that ternary compound $\text{H}_x(\text{S,C})_y$ exhibits the transition temperature within a range of $T_c = 275\text{-}287$ K (at $P = 258\text{-}270$ GPa), which is by about 5 K higher than previous record of $T_c = 280$ K, reported by Somayazulu *et al* [8] in highly-compressed LaH_{10} . While detailed phase/structural and phonon spectrum and other physical properties measurements [1-7,9,12-14], as well as the first-principle calculation studies [2,6,15-27] are on-going tasks for $\text{H}_x(\text{S,C})_y$ compound [28], in this paper we report results of the analysis of temperature dependent magnetoresistance, $R(T,B)$, from which we deduced:

1. The charge carriers effective mass, m_{eff} ;
2. The ground state superconducting coherence length, $\xi(0)$.
3. The Fermi temperature, T_F .

In a result, we find that in all considered scenarios $\text{H}_x(\text{S,C})_y$ exhibited $T_c = 190$ K ($P = 210$ GPa) has the ratio of T_c/T_F within a range of $0.011 < T_c/T_F < 0.018$. This means that $\text{H}_x(\text{S,C})_y$ falls in to unconventional superconductors band in the Uemura plot, where heavy-fermions, cuprates, pnictides and all near-room-temperature superconductors are located.

II. Description of the approach

Detailed description of the approach can be found elsewhere [29]. In short, we use the T_c/T_F ratio to locate the position of the superconductor in the Uemura plot [30]. T_F is calculated by:

$$T_F = \frac{\pi^2}{8 \cdot k_B} \cdot m_{eff}^* \cdot \xi^2(0) \cdot \left(\frac{\alpha \cdot k_B \cdot T_c}{\hbar} \right)^2, \quad (1)$$

where $\hbar = h/2\pi$ is the reduced Planck constant, k_B is the Boltzmann constant, $\alpha = \frac{2 \cdot \Delta(0)}{k_B \cdot T_c}$,

where $\Delta(0)$ is the ground state energy gap. We deduce the ground state coherence length, $\xi(0)$, by the fit of experimental $R(T, B)$ curves to analytical approximate of Werthamer, Helfand and Hohenberg theory [31,32] proposed by Baumgartner *et al* [33]:

$$B_{c2}(T) = \frac{\phi_0}{2 \cdot \pi \cdot \xi^2(0)} \cdot \left(\frac{\left(1 - \frac{T}{T_c}\right) - 0.153 \cdot \left(1 - \frac{T}{T_c}\right)^2 - 0.152 \cdot \left(1 - \frac{T}{T_c}\right)^4}{0.693} \right). \quad (2)$$

It should be noted that we define T_c and B_{c2} by employing the most strict criterion, i.e.

$\frac{R(T)}{R_{norm}} \rightarrow 0$ (detailed discussion of the problem can be found elsewhere [34]). We will

designate this model as B-WHH model.

Because $\alpha = \frac{2 \cdot \Delta(0)}{k_B \cdot T_c}$ cannot be deduced from available experimental data, we perform our calculations by assuming that α has lower and upper limits within *s*-wave superconducting gap symmetry:

$$3.5 \leq \alpha \leq 4.5 \quad (3)$$

where the lower limit is the weak-coupling limit of Bardeen-Cooper-Schrieffer theory [35] and the upper limit is the value for anharmonic phonons computed for precursor compound H₃S by first principle calculations approach [19,36].

The charge carriers effective mass, m_{eff}^* , has been calculated by the use of the Eliashberg's theory expression [37]:

$$m_{eff}^* = (1 + \lambda_{e-ph}) \cdot m_e \quad (4)$$

where m_e is the electron mass and the electron-phonon coupling constant λ_{e-ph} is deduced by the use of the advanced McMillan equations [34,38]:

$$T_c = \left(\frac{1}{1.45} \right) \cdot T_\theta \cdot e^{-\left(\frac{1.04 \cdot (1 + \lambda_{e-ph})}{\lambda_{e-ph} - \mu^* \cdot (1 + 0.62 \cdot \lambda_{e-ph})} \right)} \cdot f_1 \cdot f_2^* \quad (5)$$

where T_θ is the Debye temperature, and

$$f_1 = \left(1 + \left(\frac{\lambda_{e-ph}}{2.46 \cdot (1 + 3.8 \cdot \mu^*)} \right)^{3/2} \right)^{1/3} \quad (6)$$

$$f_2^* = 1 + (0.0241 - 0.0735 \cdot \mu^*) \cdot \lambda_{e-ph}^2. \quad (7)$$

where μ^* is the Coulomb pseudopotential parameter (ranging from $\mu^* = 0.13$ 0-0.16 [19,34,38]) for which in this paper we use an average value of $\mu^* = 0.13$. And the Debye temperature was deduced from the fit of $R(T, B = 0)$ data to Bloch-Grüneisen (BG) equation [39,40]:

$$R(T, B = 0) = R_0 + A \cdot \left(\frac{T}{T_\theta} \right)^5 \cdot \int_0^{\frac{T_\theta}{T}} \frac{x^5}{(e^x - 1) \cdot (1 - e^{-x})} \cdot dx \quad (8)$$

where T_θ , R_0 and A is a free-fitting parameter. It should be noted, that the procedure to deduce the electron-phonon coupling constant, λ_{e-ph} , by combined use of the Bloch-Grüneisen and the McMillan equations is widely used in the field [41,42].

It is important to note that analysed $R(T,B)$ datasets for $H_x(S,C)_y$ were directly extracted from Figs. 1,2 of Ref. 11 (because published $R(T,B)$ datasets are not available from the authors of Ref. 11, because these published $R(T,B)$ curves will be in use in a patent application [43]). Thus, we extract $R(T,B)$ datasets for the $H_x(S,C)_y$ samples by the use of the same routine as it has been done for dozens of $R(T,B)$ datasets for other highly-compressed superconductors, which we analysed in our recent papers [29,34]. For instance, we can mention: black phosphorous (raw data reported by Shirovani *et al* [44] in their figure 5), boron (raw data reported by Eremets *et al* [45] in their figure 2), germanium arsenide (raw data reported by Liu *et al* [46] in their figure 3), silane (raw data reported by Eremets *et al* [47] in their figure 2), ζ -phase of O_2 (raw data reported by Shimizu *et al* [48,49,50]), sulphur (raw data reported by Shimizu *et al* [51] in their Fig. 10), lithium (raw data reported by Shimizu *et al* [52] in their Fig. 2), sulphur hydride/deuteride (raw data reported by Einaga *et al* [53] in their Fig. 3(a,b); by Drozdov *et al* [1] in their figure 2(b); and by Mozaffari *et al*

[54] in their figure 1), lanthanum hydride/deuteride (raw data reported by Drozdov *et al* [55] in their figures 1,2,4, and extended data figures 2,3,5).

III. Results and discussion

Snider *et al* [11] in their Fig. 1 reported several $R(T, B = 0)$ curves for three highly-compressed $H_x(S,C)_y$ samples. To be reliably fitted to Eq. 8, the $R(T, B = 0)$ curve should be measured at reasonably wide temperature range and also should not to be distorted by any experimental artefact (for instance, the failure of electronics or diamond anvil cell, or both), which change the shape of $R(T, B)$ curve, and more likely observed drop in resistance, which can be mistakenly interpreted as the superconducting transition. We find, that from 9 presented in Figs. 1,2 [11] experimental $R(T, B=0)$ curves, the only one dataset designated as “Run 3” at $P = 210$ GPa (Fig. 1) can, with satisfaction quality, fit to Eq. 8. It should be noted that fits of other datasets to Eq. 8 either do not converge, either after the converging, deduced values have some large uncertainty boundaries, exceeding deduced values. This is a very unusual behaviour of $R(T, B=0)$ datasets for $H_x(S,C)_y$ samples reported by Snider *et al* [11], because 27 $R(T, B=0)$ datasets for a variety of highly-compressed superconductors (ranging from elements to superhydrides/superdeuterides) reported by different research groups [1,44-55] were fitted to Eq. 8 with a good quality and accuracy [29,34]. In this paper, we analyse raw $R(T, B)$ dataset for $H_x(S,C)_y$ sample (“Run 3” at $P = 210$ GPa (Fig. 1) [11]) in an assumption that this dataset is accurate and correct. However, it should be stressed that independent confirmation/disprove primary results reported by Snider *et al* [11], including very high- T_c values, is required [56].

In Fig. 1 we show the fit of $R(T, B = 0)$ curve (Run 3, $P = 210$ GPa) to Eq. 8. Deduced Debye temperature is $T_\theta = 1497 \pm 8$ K. By the use of Eqs. 5-7, and taking in account $T_c = 190$ K, one can calculate $\lambda_{e-ph} = 2.0$. This value is in a very good agreement with computed

$\lambda_{e-ph} = 1.84$ (200 GPa) and $\lambda_{e-ph} = 1.71$ (250 GPa) reported by Errea *et al* [17] for precursor binary compound H₃S. Based on pivotal result of Duan *et al* [54] who calculated $\lambda_{e-ph} = 2.19$ (200 GPa) for H₃S, we can conclude that deduced by us $\lambda_{e-ph} = 2.0$ for H_x(S,C)_y (Run 3, $P = 210$ GPa) is very close to λ_{e-ph} for binary H₃S compound. This results may allude that sample “Run 3” at $P = 210$ GPa (Fig. 1) [11] can be just binary H₃S compound. Based on deduced λ_{e-ph} value, the charge carriers effective mass is:

$$m_{eff}^* = (1 + \lambda_{e-ph}) \cdot m_e = 3.0 \cdot m_e \quad (9)$$

It should be noted that this value is in a good agreement with $m_{eff}^* = 2.76 \cdot m_e$ reported by Durajski [16] for the precursor compound H₃S.

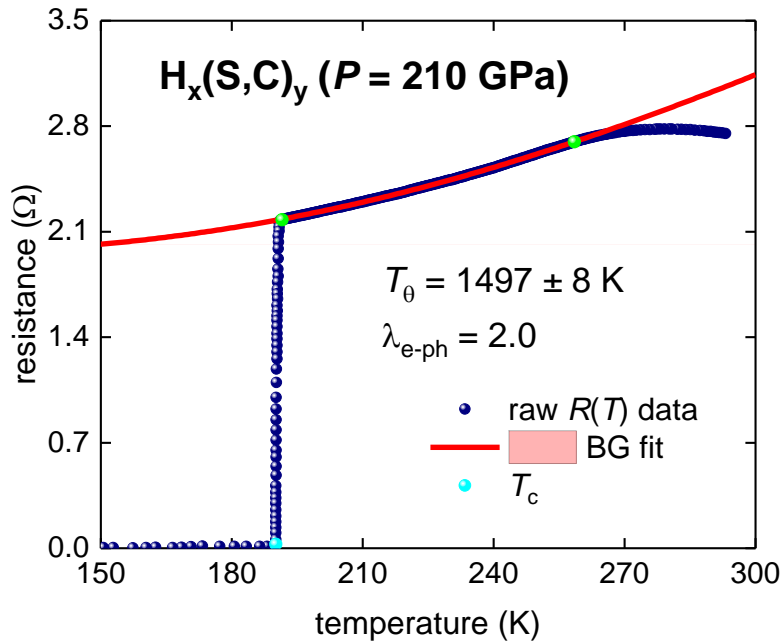


Figure 1. Resistance data, $R(T)$, and fit to BG model (Eq. 8) for H_x(S,C)_y sample compressed at $P = 210$ GPa (raw data is from Ref. 11, where the sample designated as *Run 3*). The fit quality is $R = 0.9998$. 95% confidence bar is shown. Green balls show bounds for which $R(T)$ data was used for the Eq. 8 fit.

Snider *et al* [11] in their Fig. 2(b) reported $B_{c2}(T)$ data for this sample. We extract $B_{c2}(T)$ data directly from Fig. 2(b) of Ref. 11. The fit of $B_{c2}(T)$ to Eq. 2 is shown in Fig. 2(a).

Deduced ground state coherence length is $\xi(0) = 2.39 \pm 0.04$ nm. It should be noted that

Eq. 2 is a good extrapolative tool, that can be proved for the case of highly-compressed LaH₁₀. Drozdov *et al.* [9] reported first $B_{c2}(T)$ dataset for this NRT superconductor for applied field up to $B_{\text{appl}} = 9$ T. This dataset was used to extrapolate $B_{c2}(0)$ value for LaH₁₀ in Ref. [57]. Recently, Sun et al [58] report new experimental $B_{c2}(T)$ dataset for LaH₁₀, which was measured on the world-top magnetic field facilities with applied field up to $B_{\text{appl}} = 60$ T. It can be seen that new experimental data is pretty much reproduced extrapolated values obtained by the use of Eq. 2 for dataset measured up to $B_{\text{appl}} = 9$ T in Ref. 9.

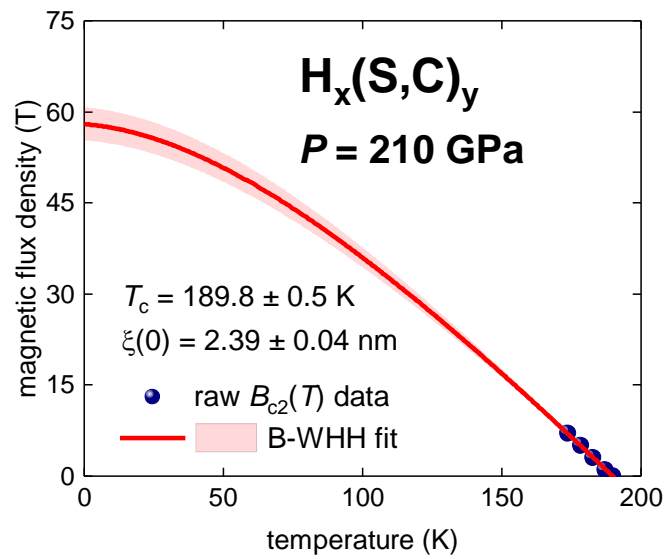


Figure 2. Superconducting upper critical field, $B_{c2}(T)$, and data fit to B-WWH model (Eq. 2) for two $H_x(S,C)_y$ samples compressed at $P = 210$ GPa (raw data is from Ref. 11). The fit quality is $R = 0.9993$. 95% confidence bars are shown.

From deduced $\xi(0)$, m_{eff}^* , and T_c , we calculate value ranges for T_F and T_c/T_F , by assuming α within its upper and lower limits (Eq. 3). The results are in Table 1.

Table I. Deduced and calculated parameters for carbonaceous sulfur hydride. For calculations we use deduced $m_{eff}^* = 3.0 \cdot m_e$.

Pressure (GPa)	Deduced T_c (K)	Deduced $\xi(0)$ (nm)	Assumed $\frac{2 \cdot \Delta(0)}{k_B \cdot T_c}$	T_F (10^4 K)	T_c/T_F
210	189.8 ± 0.5	2.39 ± 0.04	3.5	1.05 ± 0.03	0.018 ± 0.001
			4.5	1.74 ± 0.06	0.011 ± 0.001

Analysed sample of highly-compressed $H_x(S,C)_y$ are shown in the Uemura plot (Fig. 3). It can be seen, that in all considered scenarios the carbonaceous sulfur hydride has $0.011 \leq T_c/T_F \leq 0.018$ and falls in the unconventional superconductors band, where heavy-fermions, pnictides, cuprates and highly-compressed near-room-temperature superconductors are located.

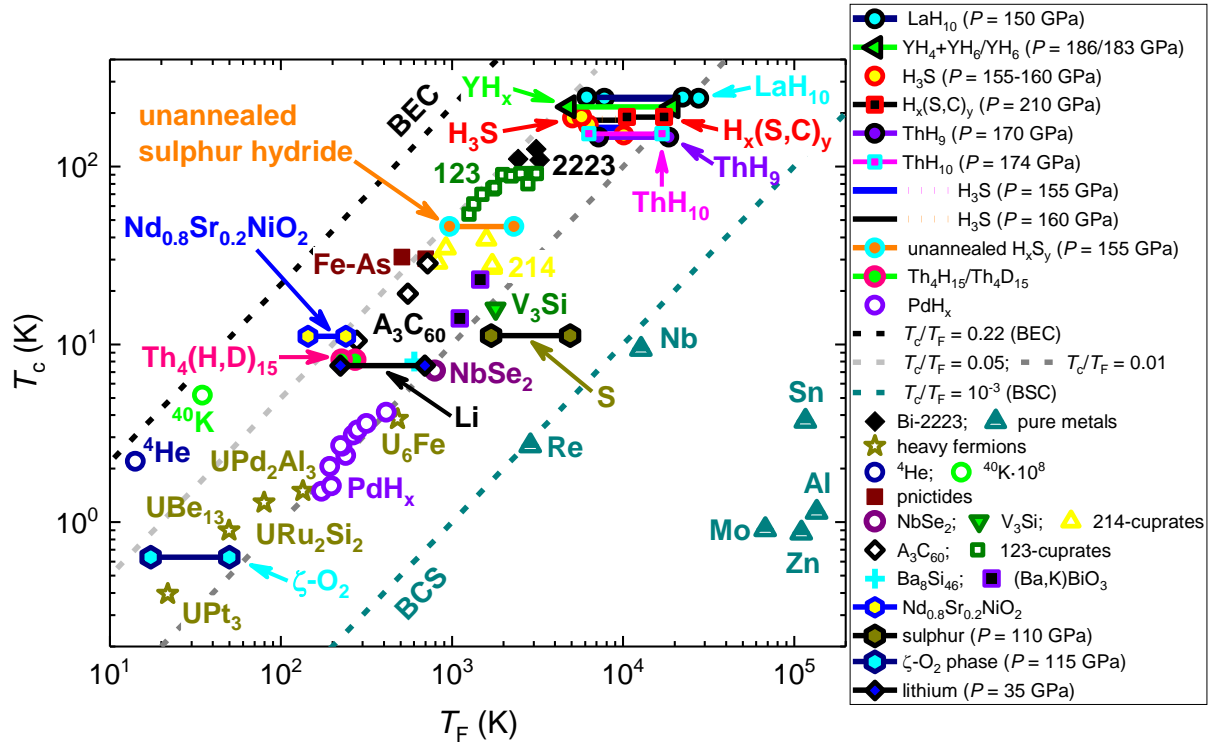


Figure 3. A plot of T_c versus T_F where $H_x(S,C)_y$ sample (red/black squares) is shown together with main superconducting families: elemental superconductors, heavy-fermions, pnictides, cuprates, and near-room-temperature superconductors. References on raw data can be found in Refs. 29,30,58,60-63. Boundary lines for the Bose-Einstein condensate (BEC), the Bardeen-Cooper-Schrieffer (BCS) superconductors, and for ratio of $T_c/T_F = 0.05$, 0.01 are shown for clarity.

There is also a need to clarify that the London penetration depth, $\lambda(T)$, for which Snider *et al* [11] calculate the value of $\lambda(0) = 2$ nm, cannot be derived in a way presented in Extended Data Fig. 3,b [11]. The estimation for $\lambda(0)$ can be made by taking in account that practically all non-elemental superconductors are type-II superconductors, and most of them have the Ginsburg-Landau parameter $\kappa(0) = \frac{\lambda(0)}{\xi(0)}$ within a range of $60 < \kappa(0) < 120$ [64-71]. Based on

deduced $\xi(0) = 2.4$ nm, expected value for $\lambda(0)$ is within a range: $144 \text{ nm} < \lambda(0) < 290 \text{ nm}$. It should be noted that binary highly-compressed H_3S has $\lambda(0) = 188 \text{ nm}$ [71].

The amplitude of the ground state superconducting gap, $\Delta(0)$, also cannot be calculated in a way, as proposed by Snider *et al* [11]. The estimate can be obtained by the use of Eq. 3, from which one can obtain: $29 \text{ meV} < \Delta(0) < 37 \text{ meV}$. It should be noted that temperature and field dependences of superconducting gap, $\Delta(T, B)$, cannot be calculated by the equation:

$$\Delta(T) = \Delta(0) \cdot 1.76 \cdot k_B \cdot T_c \cdot \sqrt{\left(1 - \frac{T}{T_c}\right)}, \quad (10)$$

which was used by Snider *et al* [11] in their Extended Data Fig. 3,d. An accurate analytical expression for $\Delta(T, B=0)$ for s -wave symmetry has been given by Gross-Alltag *et al* [72]:

$$\Delta(T) = \Delta(0) \cdot \tanh \left[\frac{\pi \cdot k_B \cdot T_c}{\Delta(0)} \cdot \sqrt{\eta \cdot \frac{\Delta C}{c} \cdot \left(\frac{T_c}{T} - 1\right)} \right] = \Delta(0) \cdot \tanh \left[\frac{2 \cdot \pi}{\alpha} \cdot \sqrt{\eta \cdot \frac{\Delta C}{c} \cdot \left(\frac{T_c}{T} - 1\right)} \right], \quad (11)$$

where $\Delta C/C$ is the relative jump in electronic specific heat at T_c , and $\eta = 2/3$.

IV. Conclusions

The discovery of superconductivity in highly-compressed H_3S by Drozdov *et al* [1] heralded the era of room-temperature superconductivity. To date, several superhydride/superdeuteride superconductors have been synthesised: BaH_{12} [25], PrH_9 [73], $\text{ThH}_9/\text{ThH}_{10}$ [2], YH_4/YH_6 [6,7], $\text{LaH}_{10}/\text{LaD}_{11}$ [8,9,14], $\text{H}_x(\text{S,C})_y$ [11]. The latter compound, in accordance with recent report by Snider *et al* [11], exhibits $T_c = 280 \text{ K}$ at pressure of $P = 267 \text{ GPa}$, which is 5 K higher than $T_c = 280 \text{ K}$ in LaH_{10} ($P = 195 \text{ GPa}$) reported by Somayazulu *et al* [8]. In this paper we extract data reported in Figs. 1,2 of Ref. 11 and deduce the electron-phonon coupling constant, $\lambda_{\text{e-ph}} = 2.0$, the ground state coherence length, $\xi(0) = 2.20 \pm 0.09 \text{ nm}$, and the Fermi temperature, $T_F = (1.7-2.8) 10^4 \text{ K}$, for the $\text{H}_x(\text{S,C})_y$ superconductor with $T_c = 190 \text{ K}$. Deduced values and reported T_c are indistinguishably close to values reported previously for primary binary compound of H_3S . From deduced values, we

calculate the T_c/T_F ratio in $H_x(S,C)_y$ compound ($T_c = 190$ K) and find that in all considered scenarios this compound should be classified as unconventional superconductors.

We should stress that our analysis reveals significant problems with all reported by Snider *et al* [11] $R(T,B)$ data for which claimed $T_c > 200$ K. These findings are in a good accord with results of independent analysis of $R(T,B)$ data reported by Hirsch and Marsiglio [56]. Based on this, independent confirmation/disprove high- T_c values in highly-compressed $H_x(S,C)_y$ is required.

Acknowledgement

Author thanks financial support provided by the state assignment of Minobrnauki of Russia (theme “Pressure” No. AAAA-A18-118020190104-3) and by Act 211 Government of the Russian Federation, contract No. 02.A03.21.0006.

References

- [1] Drozdov A P, Eremets M I, Troyan I A, Ksenofontov V, Shylin S I 2015 Conventional superconductivity at 203 kelvin at high pressures in the sulfur hydride system *Nature* **525** 73-76
- [2] Semenov D V, Kvashnin A G, Ivanova A G, Svitlyk V, Fomin V Yu, Sadakov A V, Sobolevskiy O A, Pudalov V M, Troyan I A and Oganov A R 2020 *Materials Today* **33** 36-44
- [3] Einaga M, *et al* 2016 Crystal structure of the superconducting phase of sulfur hydride *Nature Physics* **12** 835-838
- [4] Minkov V S, Prakapenka V B, Greenberg E, Eremets M I 2020 Boosted T_c of 166 K in superconducting D_3S synthesized from elemental sulfur and hydrogen *Angew. Chem. Int. Ed.* **59** 18970-18974
- [5] Matsumoto R, *et al.* 2020 Electrical transport measurements for superconducting sulfur hydrides using boron-doped diamond electrodes on beveled diamond anvil *Superconductor Science and Technology* **33** 124005
- [6] Troyan I A, *et al.* 2019 Synthesis and superconductivity of yttrium hexahydride $Im\bar{3}m$ - YH_6 *arXiv:1908.01534*
- [7] Kong P P, *et al.* 2019 Superconductivity up to 243 K in yttrium hydrides under high pressure *arXiv:1909.10482*
- [8] Somayazulu M, *et al.* 2019 Evidence for superconductivity above 260 K in lanthanum superhydride at megabar pressures *Phys. Rev. Lett.* **122** 027001
- [9] Drozdov A P, *et al* 2019 Superconductivity at 250 K in lanthanum hydride under high pressures *Nature* **569** 528-531

- [10] Sakata M, *et al.* 2020 Superconductivity of lanthanum hydride synthesized using AlH_3 as a hydrogen source *Superconductor Science and Technology* **33** 114004
- [11] Snider E, *et al.* 2020 Room-temperature superconductivity in a carbonaceous sulfur hydride *Nature* **586** 373-377
- [12] Souliou S M, Bosak A, Garbarino G and Tacon M L 2020 Inelastic x-ray scattering studies of phonon dispersions in superconductors at high pressures *Superconductor Science and Technology* **33** 124004
- [13] Laniel D, *et al* 2020 Novel sulfur hydrides synthesized at extreme conditions *Phys. Rev. B* **102** 134109
- [14] Hong F, *et al* 2020 Superconductivity of lanthanum superhydride investigated using the standard four-probe configuration under high pressures *Chinese Physics Letters* **37** 107401
- [15] Errea I, *et al* 2020 Quantum crystal structure in the 250-kelvin superconducting lanthanum hydride *Nature* **578** 66-69
- [16] Heil C, di Cataldo S, Bachelet G B and Boeri L 2019 Superconductivity in sodalite-like yttrium hydride clathrates *Physical Review B* **99** 220502(R)
- [17] Durajski A P 2016 Quantitative analysis of nonadiabatic effects in dense H_3S and PH_3 superconductors *Sci. Rep.* **6** 38570
- [18] Liu H, Naumov I I, Hoffmann R, Ashcroft N W and Hemley R J 2017 Potential high- T_c superconducting lanthanum and yttrium hydrides at high pressure *PNAS* **114** 6990-6995
- [19] Errea I *et al* 2015 High-pressure hydrogen sulfide from first principles: A strongly anharmonic phonon-mediated superconductor *Phys. Rev. Lett.* **114** 157004
- [20] Durajski A P and Szcześniak R 2018 Structural, electronic, vibrational, and superconducting properties of hydrogenated chlorine *J. Chem. Phys.* **149** 074101
- [21] Chen J, Cui W, Shi J, Xu M, Hao J, Durajski A P, and Li Y 2019 Computational design of novel hydrogen-rich YS–H compounds *ACS Omega* **4** 14317-14323
- [22] Alarco J A, Talbot P C and Mackinnon I D R 2018 Identification of superconductivity mechanisms and prediction of new materials using Density Functional Theory (DFT) calculations *J. Phys.: Conf. Ser.* **1143** 012028
- [23] Semenok D V, Kvashnin A G, Kruglov I A, and Oganov A R 2018 Actinium hydrides AcH_{10} , AcH_{12} , and AcH_{16} as high-temperature conventional superconductors *J. Phys. Chem. Lett.* **9** 1920-1926
- [24] Sun Y, Lv J, Xie Y, Liu H, and Ma Y 2019 Route to a superconducting phase above room temperature in electron-doped hydride compounds under high pressure *Phys. Rev. Lett.* **123** 097001
- [25] Chen W, *et al.* 2020 High-pressure synthesis of barium superhydrides: Pseudocubic BaH_{12} *arXiv*: 2004.12294
- [26] Ishikawa T 2020 Superconductivity of hydrogen superoxide under high pressure *Superconductor Science and Technology* **33** 114003
- [27] Shorikov A O, Skorniyakov S L, Anisimov V I and Oganov A R 2020 Electronic correlations in uranium hydride UH_5 under pressure *J. Phys.: Condens. Matter* **32** 385602
- [28] Castelvechi D 2020 First room-temperature superconductor excites - and baffles – scientists *Nature* **586** 349
- [29] Talantsev E F 2020 An approach to identifying unconventional superconductivity in highly-compressed superconductors *Superconductor Science and Technology* **33** 124001
- [30] Uemura Y J 1997 Bose-Einstein to BCS crossover picture for high- T_c cuprates *Physica C* **282-287** 194-197
- [31] Helfand E and Werthamer N R 1966 Temperature and purity dependence of the superconducting critical field, H_{c2} . II. *Phys. Rev.* **147** 288-294

- [32] Werthamer N R, Helfand E and Hohenberg P C 1966 Temperature and purity dependence of the superconducting critical field, H_{c2} . III. Electron spin and spin-orbit effects *Phys. Rev.* **147** 295-302
- [33] Baumgartner T, Eisterer M, Weber H W, Fluekiger R, Scheuerlein C, Bottura L 2014 Effects of neutron irradiation on pinning force scaling in state-of-the-art Nb₃Sn wires *Supercond. Sci. Technol.* **27** 015005
- [34] Talantsev E F 2020 Advanced McMillan's equation and its application for the analysis of highly-compressed superconductors *Superconductor Science and Technology* **33** 094009
- [35] Bardeen J, Cooper L N, Schrieffer J R 1957 Theory of superconductivity *Phys. Rev.* **108** 1175-1204
- [36] Nicol E J and Carbotte J P 2015 Comparison of pressurized sulfur hydride with conventional superconductors *Phys Rev B* **91** 220507(R)
- [37] Eliashberg G M 1960 Interactions between electrons and lattice vibrations in a superconductor *Soviet Phys. JETP* **11** 696-702
- [38] McMillan W L 1968 Transition temperature of strong-coupled superconductors *Phys. Rev.* **167** 331-344
- [39] Bloch F 1930 Zum elektrischen Widerstandsgesetz bei tiefen Temperaturen *Z. Phys.* **59** 208-214
- [40] Blatt F J 1968 *Physics of Electronic Conduction in Solids* (New York: McGraw-Hill) p. 185-190
- [41] Shang T, Philippe J, Verezhak J A T, Guguchia Z, Zhao J Z, Chang L-J, Lee M K, Gawryluk D J, Pomjakushina E, Shi M 2019 Nodeless superconductivity and preserved time-reversal symmetry in the noncentrosymmetric Mo₃P superconductor *Phys. Rev. B* **99** 184513
- [42] Matsumoto R, *et al.* 2019 Pressure-induced superconductivity in tin sulphide *Phys. Rev. B* **99** 184502
- [43] Dias R, *private communication* by e-mail on November 16, 2020 sent from verified e-mail: rdias@rochester.edu with a copy sent to verified e-mail: tobias.roedel@nature.com
- [44] Shirotani I, *et al* 1994 Phase transitions and superconductivity of black phosphorus and phosphorus-arsenic alloys at low temperatures and high pressures *Phys. Rev. B* **50** 16274-16278
- [45] Eremets M I, Struzhkin V V, Mao H-K, Hemley R J 2001 Superconductivity in boron *Science* **293** 272-274
- [46] Liu L, Struzhkin V V, Ying J 2019 Pressure-induced superconductivity in GeAs *Phys Rev B* **100** 214516
- [47] Eremets M I, Trojan I A, Medvedev S A, Tse J S, Yao Y 2008 Superconductivity in hydrogen dominant materials: Silane *Science* **319** 1506-1509
- [48] Shimizu K, Suhara K, Ikumo M, Eremets M I and Amaya K 1998 Superconductivity in oxygen *Nature* **393** 767-769
- [49] Shimizu K 2018 Superconducting elements under high pressure *Physica C* **552** 30-33
- [50] Shimizu K, Eremets M I, Suhara K, and Amaya K 1998 Oxygen under high pressure - Temperature dependence of electrical resistance *Rev. High Pressure Sci. Technol.* **7** 784-786
- [51] Shimizu K, Amaya K and Suzuki N 2005 Pressure-induced superconductivity in elemental materials *Journal of the Physical Society of Japan* **74** 1345-1357
- [52] Shimizu K, Ishikawa H, Takao D, Yagi T and Amaya K 2002 Superconductivity in compressed lithium at 20 K *Nature* **419** 597-599
- [53] Einaga M, Sakata M, Ishikawa T, Shimizu K, Eremets M I, Drozdov A P, Troyan I A, Hirao N and Ohishi Y 2016 Crystal structure of the superconducting phase of sulfur hydride *Nat. Phys.* **12** 835-8
- [54] Mozaffari S *et al* 2019 Superconducting phase diagram of H₃S under high magnetic fields *Nat. Commun.* **10** 2522

- [55] Drozdov A P et al 2019 Superconductivity at 250 K in lanthanum hydride under high pressures *Nature* **569** 528–31
- [56] Hirsch J E and Marsiglio F 2020 Absence of high temperature superconductivity in hydrides under pressure *arXiv:2010.10307*
- [57] Duan D, et al 2014 Pressure-induced metallization of dense $(\text{H}_2\text{S})_2\text{H}_2$ with high- T_c superconductivity *Sci. Rep.* **4** 6968
- [58] Talantsev E F 2019 Classifying hydrogen-rich superconductors *Materials Research Express* **6** 106002
- [59] Sun D, et al. 2020 High-temperature superconductivity on the verge of a structural instability in lanthanum superhydride *arXiv:2010.00160*
- [60] Uemura Y J 2019 Dynamic superconductivity responses in photoexcited optical conductivity and Nernst effect *Phys. Rev. Materials* **3** 104801
- [61] Ye J T, et al. 2012 Superconducting dome in a gate-tuned band insulator *Science* **338** 1193
- [62] Qian T, et al. 2011 Absence of a holelike Fermi surface for the iron-based $\text{K}_{0.8}\text{Fe}_{1.7}\text{Se}_2$ superconductor revealed by angle-resolved photoemission spectroscopy *Phys. Rev. Lett.* **106** 187001
- [63] Hashimoto K, Cho K, Shibauchi T, Kasahara S, Mizukami Y, Katsumata R, Tsuruhara Y, Terashima T, Ikeda H, Tanatar M A, Kitano H, Salovich N, Giannetta R W, Walmsley P, Carrington A, Prozorov R, Matsuda Y 2012 A sharp peak of the zero-temperature penetration depth at optimal composition in $\text{BaFe}_2(\text{As}_{1-x}\text{P}_x)_2$ *Science* **336** 1554-1557
- [64] Talantsev E F and Tallon J L 2015 Universal self-field critical current for thin-film superconductors *Nature Communications* **6** 7820
- [65] Talantsev E F, Crump W P, Tallon J L 2017 Thermodynamic parameters of single- or multi-band superconductors derived from self-field critical currents *Annalen der Physics* **529** 1700197
- [66] Sakoda M, Iida K and Naito M 2018 Recent progress in thin-film growth of Fe-based superconductors: Superior superconductivity achieved by thin films *Supercond. Sci. Technol.* **31** 093001
- [67] Iida K, Hänisch J, and Tarantini C 2018 Fe-based superconducting thin films on metallic substrates: Growth, characteristics, and relevant properties *Applied Physics Reviews* **5** 031304
- [68] Eisterer M 2018 Radiation effects on iron-based superconductors *Supercond. Sci. Technol.* **31** 013001
- [69] Kauffmann-Weiss S et al. 2019 Microscopic origin of highly enhanced current carrying capabilities of thin $\text{NdFeAs}(\text{O},\text{F})$ films *Nanoscale Advances* **1** 147
- [70] Hänisch J et al. 2019 Fe-based superconducting thin films – Preparation and tuning of superconducting properties *Supercond. Sci. Technol.* **32** 093001
- [71] Talantsev E F, Crump W P, Storey J G and Tallon J L 2017 London penetration depth and thermal fluctuations in the sulphur hydride 203 K superconductor *Annalen der Physics* **529** 1600390
- [72] Gross-Alltag F, Chandrasekhar B S, Einzel D, Hirschfeld P J, Andres K 1991 London field penetration in heavy fermion superconductors *Z. Phys. B - Condensed Matter* **82** 243-255
- [73] Zhou D, Semenok D V, Duan D, Xie H, Chen W, Huang X, Li X, Liu B, Oganov A R, Cui T 2020 Superconducting praseodymium superhydrides *Science Advances* **6** eaax6849